J Nanopart Res (2013) 15:1536
DOI 10.1007/s11051-013-1536-2

RESEARCH PAPER

Silver nanoparticles delivery system based on natural rubber latex membranes

Éder José Guidelli · Angela Kinoshita · Ana Paula Ramos · Oswaldo Baffa

Received: 21 November 2012 / Accepted: 23 February 2013 / Published online: 10 March 2013

Abstract The search for new materials for biomedical applications is extremely important. Here, we present results on the performance of a silver nanoparticles delivery system using natural rubber latex (NRL) as the polymeric matrix. Our aim was to obtain an optimized wound dressing by combining materials with potential healing action. The synthesis of silver nanoparticles and their characterization by UV–Vis spectroscopy, transmission electron microscopy, zeta potential, dynamic light scattering, and Fourier transform infrared spectroscopy (FTIR) are depicted. The NRL membranes are good matrix for silver nanoparticles and allow for their gradual release. The release of 30 nm silver nanoparticles by the NRL membranes depends on their mass percentage in NRL membranes. The total concentration of AgNP released by the NRL membranes was calculated. The AgNP attached to the *cis*-isoprene molecules in the NRL matrix remain attached to the membrane ($\sim$0.1 % w/w). So, only the AgNP bound to the non-rubber molecules are released. FTIR spectra suggest that non-rubber molecules, like aminoacids and proteins, associated with the serum fraction of the NRL may be attached to the surfaces of the released nanoparticles, thereby increasing the release of such molecules. The released silver nanoparticles are sterically stabilized, more stable and well dispersed. Because the serum fraction of the NRL is responsible for the angiogenic properties of the matrix, the silver nanoparticles could increment the angiogenic properties of NRL. This biomaterial has desirable properties for the fabrication of a wound dressing with potential healing action, since it combines the angiogenic and antibacterial properties of the silver nanoparticles with the increased angiogenic properties of the NRL.

Keywords Natural rubber latex · Drug delivery system · Silver nanoparticles · Wound dressing

É. J. Guidelli (✉) · O. Baffa
Universidade de São Paulo/FFCLRP-DF,
Ribeirão Preto, Brazil
e-mail: ederguidelli@gmail.com;
ederguidelli@pg.ffclrp.usp.br

A. Kinoshita
Universidade do Sagrado Coração, Bauru, Brazil

A. P. Ramos
Universidade de São Paulo/FFCLRP-DQ,
Ribeirão Preto, Brazil

Introduction

The search for new materials for biomedical applications is extremely important (Amsden 2003; Guidelli et al. 2011a, 2012a, b, d; Helaly et al. 1999, 2001; Park et al. 2012; Sadatmousavi et al. 2012). In this sense, natural rubber latex (NRL) extracted from *Hevea brasiliensis* has been investigated due to its wound healing properties (Ereno et al. 2010; Mrue et al. 2004;

Thomazini et al. 1997). NRL consists of approximately 45 % of a naturally occurring form of *cis*-1,4 polyisoprene; 50 % of water; and 5 % of proteins, lipids, and carbohydrates (Ferreira et al. 2009). It performs biologic actions that promotes angiogenesis (Ferreira et al. 2009; Mendonca et al. 2010), which is an important phenomenon involved in normal growth and wound healing processes. Therefore, NLR successfully functions as a curative bandage in diabetic patient's ulcers, where it induces angiogenesis and neotissue formation (Frade et al. 2001). Besides its application in the acceleration of skin cicatrization, can also be used as an occlusive membrane for guided bone regeneration (Ereno et al. 2010), as a polymeric matrix for protein delivery systems (Herculano et al. 2009), as biomaterial in vascular prosthesis fabrication (Neves-Junior et al. 2006). It also has more ordinary industrial applications, such as the fabrication of tires, condoms, and surgical gloves (Hasma et al. 2003).

The antimicrobial properties of silver nanoparticles are largely described in the literature. Silver nanoparticles are efficient antibacterial agent against *Vibrio cholera* (Krishnaraj et al. 2010), *Escherichia coli* (Krishnaraj et al. 2010), and *Staphylococcus* (Rai et al. 2009). They also exhibit cytoprotective activities toward HIV-1-infected cells (Sun et al. 2005). Their antibacterial effect is possibly due to blockage of the respiratory enzyme pathways and alterations of the cell wall and microbial DNA (Modak and Fox 1973). Thus, silver nanoparticles are an important nanomaterial for the development of wound dressing (Kwan et al. 2011; Lu et al. 2008). Besides protecting the wound from infectious contamination by microorganisms, silver nanoparticles promote wound healing and reduce scar manifestation (Tian et al. 2007). These nanoparticles possibly diminish inflammation via cytokine modulation (Tian et al. 2007).

In this context, the benefits of a biohybrid latex membrane containing silver nanoparticles for use as wound dressing can be enormous. NRL has already been used for the synthesis of silver nanoparticle (Guidelli et al. 2011b). The binding of the *cis*-isoprene molecules onto the surface of the nanoparticles is responsible for the stabilization of the particles against agglomeration and oxidation (Guidelli et al. 2011b). However, the silver nanoparticles need to be released from the NRL membranes and penetrate the wound, to perform its healing actions. This paper presents some results on the fabrication of a delivery system containing silver nanoparticles using NRL membranes (NRL–AgNP). We will show that the NRL membranes successfully accommodate the silver nanoparticles and liberate them in a time-controlled way. The released silver nanoparticles were investigated by UV–Vis spectroscopy, transmission electron microscopy (TEM), dynamic light scattering (DLS), zeta potential, and Fourier transform infrared (FTIR) spectroscopy. The NRL–AgNP membranes can be used as a delivery system of silver nanoparticles for future applications as wound dressing with potential healing properties.

Materials and methods

Materials

Silver nitrate (99.8 %) was purchased from Cennabras (Brazil). The NRL used in this study, consisted of a mix of an extract of several clones of *H. brasiliensis* and was provided by BDF Com Prod Agrícolas LTDA. After extraction, the pH was adjusted to 10 with ammonium hydroxide (NH_4OH), in order to avoid coagulation. The solution was centrifuged at $8{,}000 \times g$, to reduce the amount of allergenic proteins (Neves-Junior et al. 2006). The final product was kept in a freezer at temperatures around 8 °C.

Methods

Silver nanoparticles (AgNP) were synthesized by the chemical reduction of silver nitrate ($AgNO_3$) using sodium borohydride ($NaBH_4$). To this end, 200 mL of a 4 mM $NaBH_4$ solution was added to 200 mL of a 2 mM $AgNO_3$ solution (Guidelli et al. 2012c). The color of the solution became immediately yellow, indicating the formation of colloidal silver. The system was kept under vigorous stirring for 12 h. Then, different volumes of the solution containing AgNP were added to 8 mL of NRL, to prepare the NRL–AgNP system with different silver mass. The mixture was stirred for 5 min. The membranes were fabricated by carefully dropping the freshly prepared colloidal dispersion on a 8.5 cm diameter plate followed by drying procedure at 40 °C. To insure higher homogeneity of the membrane, the dispersion was dropped in 10 steps. The final membranes were yellow, suggesting that the AgNP were stabilized by

the rubber molecules and did not segregate to form aggregates. A pure NRL membrane was also prepared by the same procedure, as control.

Four samples containing different amounts of AgNP were produced. They were labeled according to the mass percentage of nanoparticles. For instances, NRL–AgNP_0.01 % refers to an NRL membrane containing 0.01 % silver mass percentage, and so on.

Characterization techniques

Silver nanoparticles

UV–Vis electronic absorption spectra of the colloidal dispersions were recorded using an Ultrospec 2100 pro (Amersham Pharmacia) spectrophotometer. AgNP morphology and size were investigated by TEM using a JEOL-JEM-100 CXII instrument. A drop of the colloidal dispersion onto a copper grid covered with a conductive polymer was dried.

NRL–AgNP delivery system

To obtain the AgNp release rate, the pure NRL membranes and the NRL–AgNP delivery systems were individually immersed in a flask containing 20 mL of Mili-Q^{TM} water. Then, 2 mL of each solution were collected for UV–Vis spectroscopy experiments. The spectra of solutions containing immersed NRL–AgNP were acquired using the solution containing immersed pure NRL membrane as reference, to subtract any possible absorption bands arising from molecules released by the NRL membrane, and insure that only the plasmon absorption band of the AgNP was accounted for. After the UV–Vis spectrum was registered, the aliquot was returned to the flask, to avoid alteration in the total volume of water. This procedure was repeated several times, along 48 h.

The zeta potential and the particle size distributions (PSD) were measured on a Zeta-Sizer system (Malvern Instruments). The zeta potential of the nanoparticles was measured from their electrophoretic mobility by employing a quartz capillary cell containing a pair of palladium electrodes. This dispersion was injected into the capillary of the Zeta-Sizer system and the zeta potential was measured ten times. The mean zeta potential values for three replicates were calculated. For the PSD, the data were collected at a fixed angle (90°) and fixed wavelength (633 nm He–Ne laser). FTIR spectra were acquired on a Bomem MB 100 spectrometer in the region between 4,000 and 400 cm^{-1}. The solutions containing the released compounds were dropped onto a Si ⟨100⟩ support, in order to obtain a film.

Results and discussion

Figure 1 presents the UV–Vis spectrum of the colloidal silver particles. The formation of AgNP was confirmed by the presence of the absorption plasmon peak around 390 nm (Khlebtsov 2008). This peak is characteristic of the collective oscillation of the conducting electrons in the nanoparticles surfaces in the presence of a light wave field (Khlebtsov 2008). The intensity of the peak is proportional to the AgNP concentration; the full width at half maximum is proportional to the size distribution (Medina-Ramirez et al. 2009).

Figure 2 displays the TEM images of colloidal AgNP and evidences a high degree of agglomeration. However, the agglomerates consist of small silver particles (Figire 2b). The PSD obtained by DLS indicates an average diameter of 20 nm. Bearing in mind that PSD and UV–Vis of the colloidal dispersion point to spherical AgNP with 20-nm diameter, aggregation probably occurred during drying onto the copper grid. This happened because the AgNP were

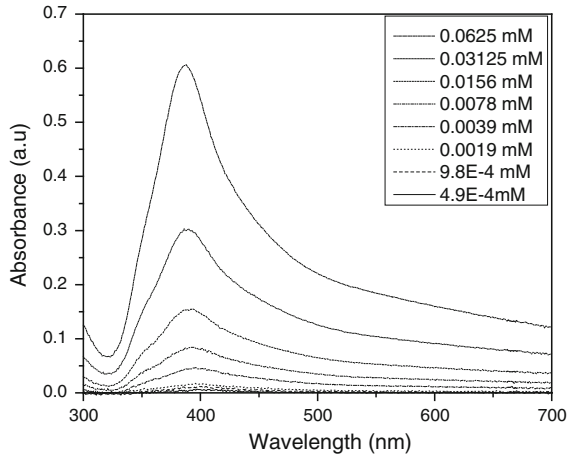

Fig. 1 UV–Vis absorption spectrum of the colloidal silver dispersion in different $AgNO_3$ concentrations

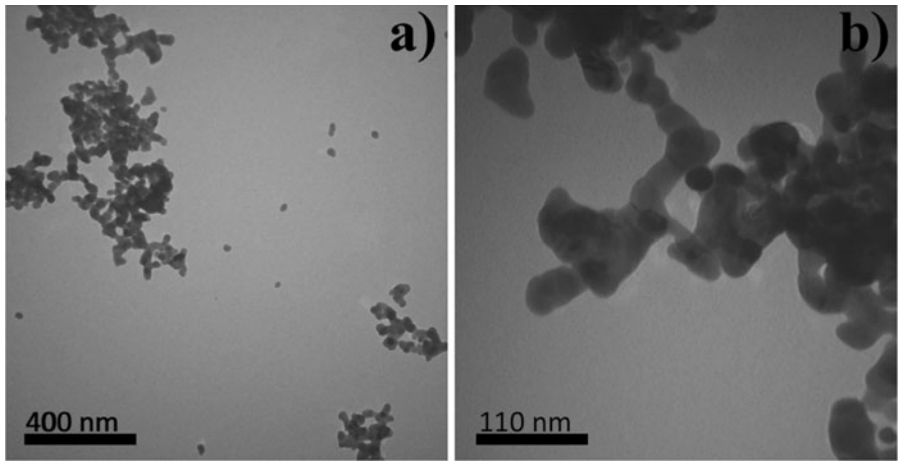

Fig. 2 TEM micrographs of the silver nanoparticles in different regions and magnifications

not capped with any passivation molecule during the synthesis.

To determine the molar absorptivity coefficient of the AgNP ($\varepsilon_{(\lambda)}$), we constructed the curve of absorbance at the plasmon peak as a function of the $AgNO_3$ molar concentration. To this end, the starting dispersion containing 1 mM $AgNO_3$ was diluted several times, and the absorption spectrum was collected for each dilution (Fig. 1).

According to the Lambert–Beer law:

$$A = \varepsilon_{(\lambda)} b C,$$

where A is the absorbance, $\varepsilon_{(\lambda)}$ is the molar absorptivity coefficient, b is the optical path, and C is the concentration. The optical path was 1 cm for all the measurements, so the slope of the calibration curve resulted in $\varepsilon_{(\text{plasmon})} = 9.57$ L mmol^{-1} cm^{-1} (Fig. 3).

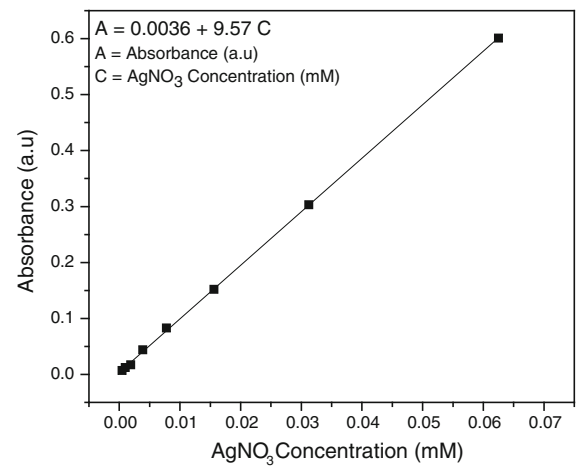

Fig. 3 Absorbance at the plasmon peak as a function of the $AgNO_3$ concentration in the colloidal silver dispersion

Figure 4 depicts the UV–Vis absorption peak of the AgNP released by the NRL membranes. The UV–Vis spectra of the sample NRL–AgNp_0.1 % do not display a clear plasmon absorption band in the first 24 h (Fig. 4a). This suggests that the AgNP were not released from the NRL–AgNP membranes or the concentration of the AgNP released was too low to be detected. In fact, plasmon band with a very low intensity could only be detected after 48 h, thereby suggesting that the AgNP are strongly bound to the NRL matrix. The binding of AgNP to the NRL matrix probably occurs via the *cis*-isoprene molecules (Guidelli et al. 2011b).

The color of the solution of the samples NRL–AgNP_0.2 % and NRL–AgNp_0.4 % became pale yellow, suggesting that the NRL matrix liberated AgNP (Fig. 4b, c). The plasmon absorption peak at 405 nm in the UV–Vis spectra of the collected aliquots revealed that AgNp is present in water (Fig. 4), confirming that the NRL membrane released the nanoparticles in the water along time. The red shift of the plasmon band from 390 to 405 nm is probably associated with particle growth and/or agglomeration, or it can be caused by the changes in the medium surrounding the AgNPs. In the case of the pure colloidal silver dispersion, the surrounding medium consists of water molecules only; in the case of the released AgNP, the medium may also contain molecules released by the NRL.

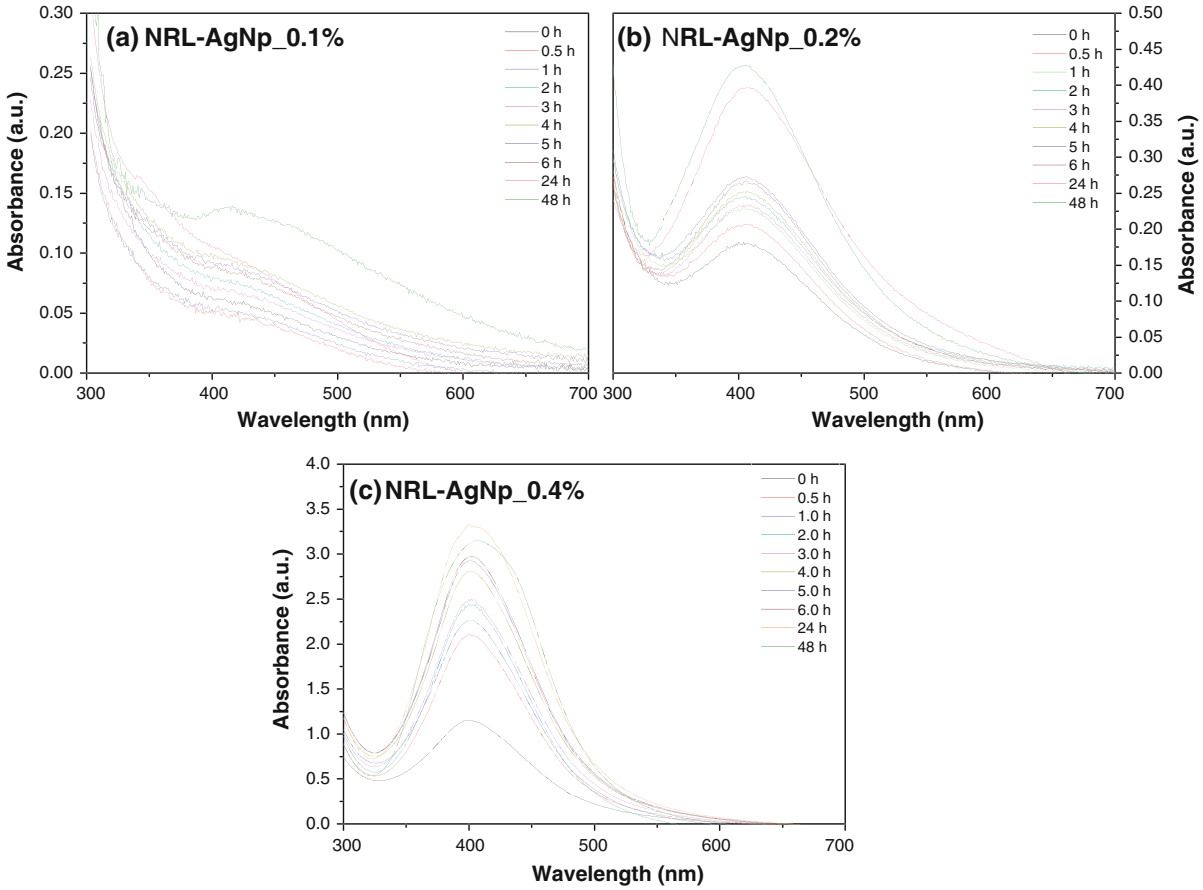

Fig. 4 UV–Vis spectra of the silver nanoparticles released by the latex membranes: **a** NRL–AgNp_0.1 %, **b** NRL–AgNp_0.2 %, and **c** NRL–AgNp_0.4 %

A very clear plasmon absorption band for the sample NRL–AgNp_0.2 % after 24 h of immersion, and the virtual absence of such plasmon for the sample AgNp_0.1 %, allow us to estimate that a mass percentage of approximately 0.1 % of AgNP remains bound to the NRL matrix. The AgNP that are released from samples NRL–AgNp_0.2 % and NRL–AgNp_0.4 %, are probably excess nanoparticles that the matrix cannot accommodate.

Figure 5 illustrates the absorbance at 405 nm (Fig. 4) as a function of time. Larger mass percentage of silver nanoparticles in the NRL membrane increases the AgNP release speed. Taking the absorbance at 405 nm after 48 h and adopting $\varepsilon_{(\text{plasmon})} = 9.57$ L mmol^{-1} cm^{-1}, as calculated above, we obtained the total concentration of AgNP released by the NRL membranes as: 1.4×10^{-5}, 4.5×10^{-5}, and 3.34×10^{-4} mol L^{-1}, for the samples NRL–AgNp_0.1 %, NRL–AgNp_0.2 %, and NRL–AgNp_0.4 %, respectively. It is noteworthy that the concentration of silver calculated for the sample NRL–AgNp_0.4 % may be underestimated, because of the high absorbance of the sample. In this condition, the large attenuation of light inside the highgly concentrated sample can invalidate the Lambert–Beer law.

Figure 6 shows the TEM images obtained from the nanoparticles released from the NRL–AgNp_0.4 % after 48 h of immersion. The released nanoparticles are spherical, uniform, well-dispersed, and have better dispersity compared with uncapped silver nanoparticles (as shown in Fig. 2).

Figure 7 contains the PSD obtained by DLS for the pure colloidal silver dispersion and for the AgNP released by the NRL–AgNp membranes. The released nanoparticles have mean size similar to that of the pure colloidal silver dispersion. Thus, the AgNPs do not

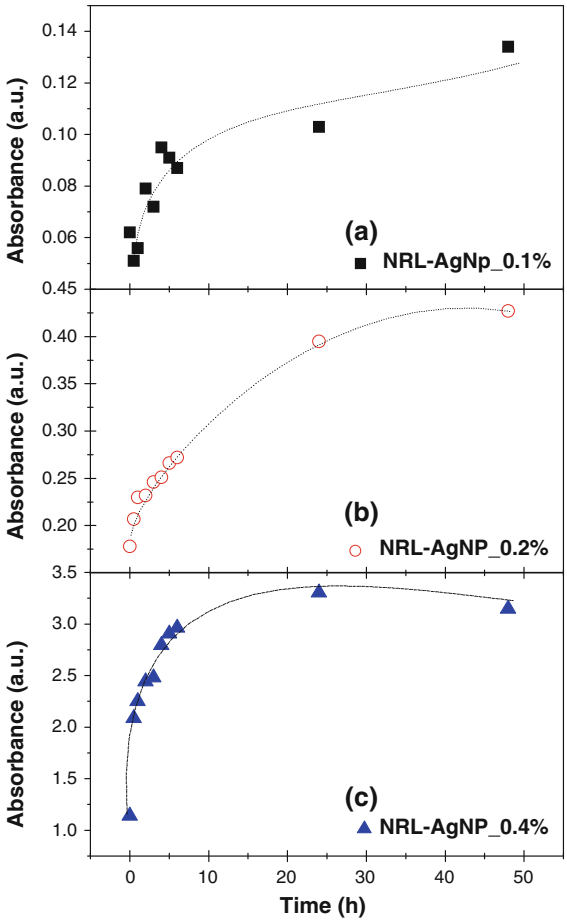

Fig. 5 Absorbance at the plasmon peak of the silver nanoparticles released by the latex membranes as a function of time

agglomerate after insertion in the NRL membranes. As a result, the NRL can be successfully used to stabilize and accommodate AgNP. The red shift of the plasmon absorption band from 390 nm, in the case of pure AgNP solution, to 405 nm, in the case of AgNP released by the NRL seems to be a consequence of changing the surrounding medium from water to water plus NRL-delivered molecules, respectively, and not due to particle agglomeration.

The zeta potential of the nanoparticles informs about the stability of the nanoparticles. Electrostatically stabilized nanoparticles exhibiting a zeta potential higher than ±20 mV are considered stable. For sterically stabilized nanoparticles, the zeta potential value does not influence the colloidal stability greatly. Table 1 lists the zeta potential of the pure colloidal AgNP dispersion and of the AgNP released from samples NRL–AgNp_0.1 %, NRL–AgNp_0.2 %, and NRL–AgNp_0.4 %. Although all the samples exhibit negative zeta potential, the AgNP released by the NRL–AgNp membranes have smaller absolute zeta potential (less negative) values than the pure colloidal AgNP dispersion. The change in the zeta potential after AgNP release corroborates surface modification of the particles due to NRL binding. The negative potential of the AgNP prepared by the chemical reduction of silver nitrate with sodium borohydride is due to adsorption of BH_4^- radicals onto the nanoparticles surfaces, which electrostatically stabilizes the AgNP (Solomon et al. 2007). Reduction of the zeta

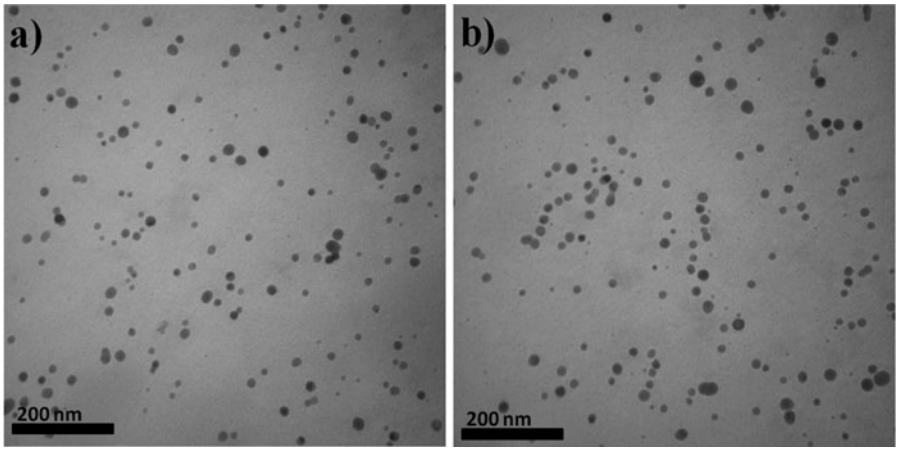

Fig. 6 TEM micrographs of the silver nanoparticles released by the sample NRL–AgNp_0.4 %

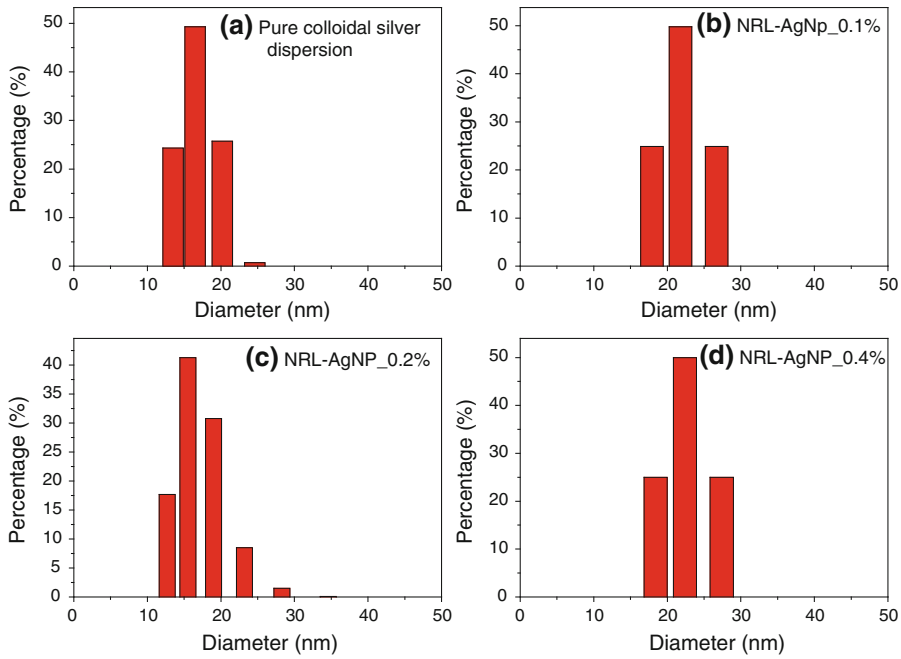

Fig. 7 Particle size distribution obtained by the dynamic light scattering technique of the **a** colloidal silver dispersion and of the silver nanoparticles released by the samples **b** NRL–AgNp_0.1 %, **c** NRL–AgNp_0.2 %, and **d** NRL–AgNp_0.4 %

potential value of the released AgNP would result in decreased colloidal stability, and culminate in particle agglomeration. However, because the AgNP released by the NRL–AgNp membranes are well-dispersed and stable in shape and size and, as evidenced by the UV–Vis spectroscopy, DLS technique, and TEM images, their lower zeta potential indicates that the released nanoparticles are also stabilized by steric repulsion. In other word, it is possible that some molecules from the NRL are attached to the nanoparticles surfaces, avoiding their agglomeration when they have reduced zeta potential.

Fourier transform infrared spectra of the solutions, where the NRL and NRL–AgNp were immersed, were recorded to investigate the possible organic compounds released by the NRL membranes and that could be attached to the AgNps. The FTIR spectra of the solutions after insertion of pure NRL and the sample NRL–AgNp_0.4 % are very similar (Fig. 8). The broad and strong peak ranging from 3,000 to 3,600 cm^{-1} is related to the overlapping of OH and NH_2 stretching vibrations. The peak at 2,922 cm^{-1} corresponds to the asymmetric stretching of the CH_2 groups. The bands in the range from 1,200 to 1,700 cm^{-1} in the spectrum of the solution containing released AgNP are very similar to the FTIR spectrum of the serum fraction isolated from the NRL (Ferreira et al. 2009). The bands at 1,650 and 1,580 cm^{-1} refer to amide I and amide II of the non-rubber constituent of latex (Ferreira et al. 2009).

Table 1 Zeta potential of the silver nanoparticles released by each sample

Sample name	Zeta potential (mV)
Pure AgNP	-36 ± 2
NRL–AgNp_0.1 %	-21 ± 2
NRL–AgNp_0.2 %	-20 ± 3
NRL–AgNp_0.4 %	-23 ± 3

Figure 8 reveals a more intense band at 1,400 cm^{-1}, in the FTIR spectrum of the sample obtained from the solution released by the sample NRL–AgNp_0.4 %, assigned to the serum fraction of the latex; i.e., its non-rubber constituents (Ferreira et al. 2009). Therefore, it seems that the AgNP drag non-rubber molecules from NRL attached to the AgNP surface. These molecules are associated with the serum fraction. These AgNP-attached non-rubber molecules may be responsible for steric stabilization, thereby increasing AgNP stability and dispersity despite the reduced zeta potential, as discussed before.

Silver nanoparticles interact with NRL films via the *cis*-isoprene molecules (Guidelli et al. 2011b). Since we did not detect the main bands associated with *cis*-isoprene in the solution released by the NRL–AgNp

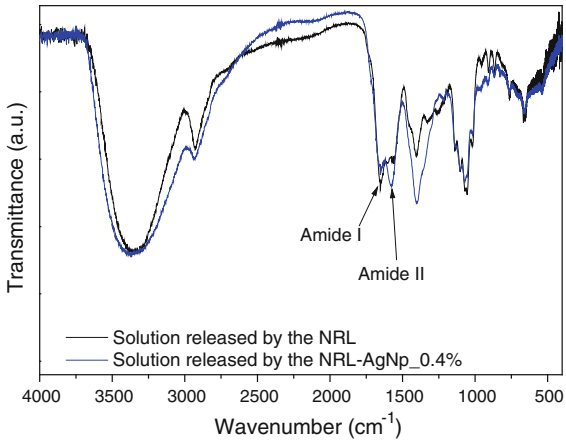

Fig. 8 FTIR spectra of the solution released by the pure NRL membrane and of the sample NRL–AgNp_0.4 %

membranes, the particles attached to the *cis*-isoprene molecules probably remain bound to the membranes. Hence, only AgNP that are not attached to the rubber molecules, i.e., the excess nanoparticles, are released. This might explain why the NRL–AgNp_0.1 % does not liberate considerable amounts of AgNP.

Because the NRL serum fraction is responsible for the angiogenic properties of the NRL extracted from *H. Brasiliensis* (Ferreira et al. 2009; Mendonca et al. 2010), we can suggest that the AgNP potentializes the angiogenic properties intrinsic to the NRL by increasing the release of molecules responsible for angiogenesis. Therefore, AgNP–NRL membranes combine the angiogenic and antibacterial properties of the separate components and gives rise to enhanced angiogenic capacity.

Conclusions

We have successfully combined silver nanoparticles and NRL to obtain a silver nanoparticle delivery system with antibacterial activity and enhanced angiogenic properties. The plasmon absorption peak detected by UV–Vis spectroscopy confirms AgNP release by the NRL–AgNp membranes. The rise in the mass percentage of AgNP in the NRL membrane increase the AgNP release rate from the membranes. The AgNP released from the samples NRL–AgNp_0.2 % and NRL–AgNp_0.4 % are probably excess nanoparticles, and silver mass percentage of approximately 0.1 % remains bound to the NRL matrix. The reduced zeta potential of the released AgNP indicates surface modification by the NRL molecules, which stabilize the AgNP from a steric viewpoint. FTIR spectra suggest that AgNP drag non-rubber molecules from NRL. These non-rubber molecules attached to the AgNP are associated with the NRL serum fraction and may be responsible for steric stabilization. The AgNP attached to the *cis*-isoprene molecules in the NRL matrix remain attached to the membrane. So, only the AgNP bound to the non-rubber molecules are released. Because the NRL serum fraction is responsible for the angiogenic properties of NRL, the silver nanoparticles could potentialize the angiogenic properties intrinsic to the NRL by increasing the release of the molecules responsible for angiogenesis. These results reveal that this biohybrid nanomaterial features properties for fabrication of a wound dressing with potential healing action. This material combines the angiogenic characteristic of NRL with the antibacterial properties of the AgNP and AgNP potentialize the NRL angiogenic activity. Future studies will focus on the influence nanoparticle size on the AgNP release rate, as well as on the tissue reaction after implant and the performance of the biohybrid material as wound dressing.

Acknowledgments The authors are grateful to C. A. Brunello for technical assistance, Professor A. S. Ito for the use of his UV–Vis spectrometer, Professor. M. E. D. Zaniquelli for the use of the zetaSizer system, and Dr. Cynthia Maria de Campos Prado Manso for language revision. This study was supported by the Brazilian agencies: FAPESP, CNPq, and CAPES.

References

Amsden B (2003) A model for osmotic pressure driven release from cylindrical rubbery polymer matrices. J Control Release 93(3):249–258

Ereno C, Catanzaro Guimaraes SA, Pasetto S, Herculano RD, Silva CP, Graeff CFO et al (2010) Latex use as an occlusive membrane for guided bone regeneration. J Biomed Mater Res A 95A(3):932–939

Ferreira M, Mendonca RJ, Coutinho-Netto J, Mulato M (2009) Angiogenic properties of natural rubber latex biomembranes and the serum fraction of *Hevea brasiliensis*. Braz J Phys 39(3):564–569

Frade MAC, Valverde RV, de Assis RVC, Coutinho-Netto J, Foss NT (2001) Chronic phlebopathic cutaneous ulcer: a therapeutic proposal. Int J Dermatol 40(3):238–240

Guidelli EJ, Guerra EM, Mulato M (2011a) Ion sensing properties of vanadium/tungsten mixed oxides. Mater Chem Phys 125(3):833–837

Guidelli EJ, Ramos AP, Zaniquelli MED, Baffa O (2011b) Green synthesis of colloidal silver nanoparticles using natural rubber latex extracted from *Hevea brasiliensis*. Spectrochim Acta A Mol Biomol Spectrosc 82(1):140–145

Guidelli EJ, Guerra EM, Mulato M (2012a) Vanadium and titanium mixed oxide films: synthesis, characterization and application as ion sensor. J Electrochem Soc 159(6):J217–J222

Guidelli EJ, Ramos AP, Zaniquelli MED, Nicolucci P, Baffa O (2012b) Synthesis and characterization of gold/alanine nanocomposites with potential properties for medical application as radiation sensors. ACS Appl Mater Interfaces 4(11):5844–5851

Guidelli EJ, Ramos AP, Zaniquelli MED, Nicolucci P, Baffa O (2012c) Synthesis and characterization of silver/alanine nanocomposites for radiation detection in medical applications: the influence of particle size on the detection properties. Nanoscale 4(9):2884–2893

Guidelli EJ, Ramos AP, Zaniquelli MED, Nicolucci P, Beffa O (2012d) Synthesis of silver nanoparticles using DL-alanine for ESR dosimetry applications. Radiat Phys Chem 81(3):301–307

Hasma H, Othman AB, Fauzi MS (2003) Barrier integrity of punctured gloves: NR superior to vinyl and nitrile. J Rubber Res 6(4):9

Helaly FM, Ahmed A, Abd El-Ghaffar MA (1999) Natural rubber base matrix containing *Calendula officinalis* plant as a source of molluscicidal saponin. J Control Release 57(1):1–7

Helaly FM, Soliman HSM, Soheir AD, Ahmed AA (2001) Controlled release of migration of molluscicidal saponin from different types of polymers containing *Calendula officinalis*. Adv Polym Technol 20(4):305–311

Herculano RD, Silva CP, Ereno C, Catanzaro Guimaraes SA, Kinoshita A, de Oliveira Graeff CF (2009) Natural rubber latex used as drug delivery system in guided bone regeneration (GBR). Mater Res Ibero Am J Mater 12(2):253–256

Khlebtsov NG (2008) Optics and biophotonics of nanoparticles with a plasmon resonance. Quantum Electron 38(6):504–529

Krishnaraj C, Jagan EG, Rajasekar S, Selvakumar P, Kalaichelvan PT, Mohan N (2010) Synthesis of silver nanoparticles using *Acalypha indica* leaf extracts and its antibacterial activity against water borne pathogens. Colloids Surf B Biointerfaces 76(1):50–56

Kwan KH, Liu X, Yeung KW (2011) Silver nanoparticles improve wound healing. Nanomedicine 6(4):595–596

Lu S, Gao W, Gu HY (2008) Construction, application and biosafety of silver nanocrystalline chitosan wound dressing. Burns 34(5):623–628

Medina-Ramirez I, Bashir S, Luo ZP, Liu JL (2009) Green synthesis and characterization of polymer-stabilized silver nanoparticles. Colloids Surf B Biointerfaces 73(2):185–191

Mendonca RJ, Mauricio VB, Teixeira LDB, Lachat JJ, Coutinho-Netto J (2010) Increased vascular permeability, angiogenesis and wound healing induced by the serum of natural latex of the rubber tree *Hevea brasiliensis*. Phytother Res 24(5):764–768

Modak SM, Fox CL (1973) Binding of silver sulfadiazine to cellular components of *Pseudomonas aeruginosa*. Biochem Pharmacol 22(19):2391–2404

Mrue F, Coutinho-Netto J, Ceneviva R, Lachat JJ, Thomazini JA, Tambelini H (2004) Evaluation of the biocompatibility of a new biomembrane. Mater Res 7(2):6

Neves-Junior WFP, Ferreira M, Alves MCO, Graeff CFO, Mulato M, Coutinho-Netto J et al (2006) Influence of fabrication process on the final properties of natural-rubber latex tubes for vascular prosthesis. Braz J Phys 36(2B):586–591

Park H-S, Seo J-A, Lee H-Y, Kim H-W, Wall IB, Gong M-S et al (2012) Synthesis of elastic biodegradable polyesters of ethylene glycol and butylene glycol from sebacic acid. Acta Biomater 8(8):2911–2918

Rai M, Yadav A, Gade A (2009) Silver nanoparticles as a new generation of antimicrobials. Biotechnol Adv 27(1):76–83

Sadatmousavi P, Mamo T, Chen P (2012) Diethylene glycol functionalized self-assembling peptide nanofibers and their hydrophobic drug delivery potential. Acta Biomater 8(9):3241–3250

Solomon SD, Bahadory M, Jeyarajasingam AV, Rutkowsky SA, Boritz C, Mulfinger L (2007) Synthesis and study of silver nanoparticles. J Chem Educ 84(2):322–325

Sun RWY, Chen R, Chung NPY, Ho CM, Lin CLS, Che CM (2005) Silver nanoparticles fabricated in Hepes buffer exhibit cytoprotective activities toward HIV-1 infected cells. Chem Commun 40:5059–5061

Thomazini JA, Mrue F, Coutinho-Netto J, Lachat JJ, Ceneviva R, Zborowski AC (1997) Morphological and biochemical characterization of a prosthesis manufactured from natural latex of *Hevea brasiliensis* for medical utilization. Acta Microscopica 6:1

Tian J, Wong KKY, Ho C-M, Lok C-N, Yu W-Y, Che C-M et al (2007) Topical delivery of silver nanoparticles promotes wound healing. ChemMedChem 2(1):129–136